

A NUMERICAL AND EXPERIMENTAL STUDY ON MOTION RESPONSES OF SEMI-SUBMERSIBLE PLATFORMS SUBJECTED TO SHORT CRESTED WAVES

V.J. Kurian*, C.Y. Ng, M.S. Liew

Universiti Teknologi PETRONAS, Tronoh, Malaysia
kurian_john@petronas.com.my
carrol.ng82@gmail.com
shahir_liew@petronas.com.my

Keywords: Short crested waves, semi-submersible platforms, hydrodynamic analysis, wave tank tests, Response amplitude operator.

Abstract. *The effect of the short-crested waves on the motions of moored semi-submersible platform is demonstrated from the results of the model tests, compared with the theoretical calculations. The model tests were performed in the wave tank located in the Offshore Laboratory of Universiti Teknologi PETRONAS. In the tests, model was moored in the head sea with four linear springs fore and aft, and the motion responses subjected to multi-directional waves were measured. The responses in three degrees of freedom (surge, heave and pitch) are presented. A time domain numerical MATLAB code, incorporated with the short-crested wave effect was developed. In each time step, the mass, damping and stiffness matrices were calculated. The diffraction of short-crested wave force on circular cylinder was adopted, and the equation of motion was solved by the Newmark Beta method. Responses in term of Response Amplitude Operator (RAO) are presented and compared. Good agreement between numerical and experimental results was achieved.*

1 INTRODUCTION

This work studied the dynamic motion responses of the six-column semisubmersible platform due to multi-directional short crested waves by numerical simulation that validated by wave tank test. One of the major concerns in design of offshore structures is the determination of environmental forces due to wind, wave and current. Among these, wave forces give the greatest challenges where it constitutes about 70% of the total environmental forces. Conventionally, two-dimensional wave or the long crested wave statistics is adopted for the design of offshore structures. Yet, waves due to wind flow in the real sea condition are short-crested. The real sea conditions are well defined by the short crested waves, where the wave properties throughout the cross section at X-Z axis are different. Hence, it is always referred as three-dimensional wave.

Even though short crested waves are appropriate to be considered for the real sea condition, majority of the studies are focused on the two-dimensional long crested waves. Study focused on regular wave force including the viscous damping effect and viscous exciting effect subjected to semisubmersible platform was presented by Sun [1]. Soylemez [2] presented a basic tool to obtain the wave forces and moments for cylindrical members of floating structures. Paulling et al [3] developed a computer system to investigate the wave induced load and motion of semisubmersible catamaran type platform, where the force was obtained by adopting strip theory that incorporated Frank's close fit two dimension procedures. A series of benchmark test for a turret moored FPSO, a classic SPAR and a standard TLP acted by the irregular long crested waves were studied [4-6]. Model tests were performed on a six-column semisubmersible platform at the operating and survival conditions by Collins and Grove [7] to provide an input for calibration and correlation studies for analytic prediction techniques, non-linear phenomena and qualitative assessment of realistic environment modeling. Natarajan and Ganapathy [8] performed model tests to study the moored ship behavior acted by wave and current.

With the increased interest in the real sea conditions, number of studies focusing on the short crested waves, has been done. One of the most significant studies in this area was performed by Zhu [9]. Zhu introduced a solution for a circular cylinder acted by the diffraction of short crested waves. In this study, he showed that the spreading of the short crested waves affected the hydrodynamic wave force, where the greater spreading yielded smaller hydrodynamic forces. Then, Zhu and Moule [10] expanded the study by incorporating various arbitrary cross sections of the circular cylinder. It was found that for certain cross sections, the short crested wave induced larger force than that by plane waves with the same total wave number. The theory by Zhu was also extended by Zhu and Satravaha [11], where they included the effects of nonlinear wave until the second order of wave amplitude. Jian et al [12] extended Zhu's theory by incorporating the effects of a uniform current for different incident angle.

Heidari et al [13] performed a study on the hydrodynamics of a moored semisubmersible subjected to the short crested wave. They developed a frequency domain analysis, which included the strip theory, effects of phase lag on the force and the response amplitude of the structure. Two theories to obtain the short crested wave field for two modes of propagation that incorporated the resonant propagation and non-resonant propagation were derived by Iou-lalen et al [14]. The short crested wave interaction with a concentric porous cylindrical structure was studied by Tao et al [15]. Zhang et al [16][17] investigated the directional wave hybrid models for the wave properties of short crested waves. Majority of the study focused on the short crested wave properties. Hereby, in this study a numerical simulation and an ex-

perimental study were performed to investigate the dynamic motion responses of the semi-submersible platform model subjected to multi-directional short crested waves.

2 NUMERICAL FORMULATIONS

A MATLAB code investigating the dynamic responses of a six-column semisubmersible platform model subjected to short crested waves that incorporated the effects of diffraction was developed. In the simulation, the model was assumed to be rigid, which restrained by mooring line at each corner. The matrices for mass, damping and stiffness were evaluated for every time step. The equation of motions for the platform dynamic equilibrium were formulated and solved by the Newmark Beta Method.

2.1 Wave kinematics

In the numerical simulation, linear airy wave theory was adopted to obtain the wave properties. In this case, the wave height is assumed to be small enough with respect to the wave length or the water depth. Furthermore, the wave height term was dropped beyond the first order to linear the free surface boundary, which satisfied the mean water level instead of the oscillating free surface. The first order velocity potential is given as

$$\phi = \frac{gH}{2\omega} \frac{\cosh k(z+d)}{\cosh(kd)} \sin\theta \quad (1)$$

where g = gravitational acceleration, H = wave height, ω = wave frequency ($\omega = 2\pi/T$), k = wave number ($k = 2\pi/L$), T = wave period, L = wave length.

The water particle velocities and acceleration in horizontal and vertical axis are given as

$$u = \frac{\pi H}{T} \frac{\cosh k(z+d)}{\sinh(kd)} \cos\theta \quad (2)$$

$$v = \frac{\pi H}{T} \frac{\sinh k(z+d)}{\sinh(kd)} \sin\theta \quad (3)$$

$$\frac{\partial u}{\partial t} = \frac{2\pi^2 H}{T^2} \frac{\cosh k(z+d)}{\sinh(kd)} \sin\theta \quad (4)$$

$$\frac{\partial v}{\partial t} = -\frac{2\pi^2 H}{T^2} \frac{\sinh k(z+d)}{\sinh(kd)} \cos\theta \quad (5)$$

where z = vertical coordinate, $\theta = kx - \omega t$.

2.2 Diffraction short crested waves forces

By considering the real sea conditions, Zhu's theory was modified. In Zhu's theory, the assumption was made, where the water run-up and pressure distribution were taken around the bottom seated cylinder. The concept of the theory was implemented by considering the surge diffraction force as a product obtained from integrating the total length of the vertical columns. The surge diffraction force for the vertical columns of the semisubmersible is given as:

$$F_{x \text{ column}} = \int_{-h}^0 \frac{dF_z}{dz} dz \quad (6)$$

$$F_{x \text{ column}} = \int_{-h}^0 -2\pi\rho g r H \frac{\cosh k(z+d)}{\cosh kd} e^{-i\omega t} R(k_x, k_y, k, r) dz \quad (7)$$

where

$$R(k_x, k_y, k, r) = i [R_0(k_x, k_y, k, r) + \sum_{n=1}^{\infty} R_n(k_x, k_y, k, r)] \quad (8)$$

$$R_0(k_x, k_y, k, r) = J_1(k_x r) J_0(k_y r) - \frac{k_x J_1(k_x r) J_0(k_y r) + k_y J_1(k_x r) J_0(k_y r)}{k H_1(kr)} H_1(kr) \quad (9)$$

$$R_n(k_x, k_y, k, r) = i^{2n} \begin{Bmatrix} [J_{2n+1}(k_x r) J_{2n}(k_y r) - B_{2n+1} H_1(kr)] \\ [J_{2n-1}(k_x r) J_{2n}(k_y r) - B_{2n-1} H_1(kr)] \end{Bmatrix} \quad (10)$$

To obtain the heave force, the dynamic pressure on the bottom surface of the pontoon hull, which derived from the Bernoulli equation and potential velocity was double integrated. The total pitch moment about the axis parallel to the y-axis passing through the bottom of the column is given as

$$M_{y \text{ column}} = \int_{-h}^0 (z+d) F_{x \text{ column}} dz \quad (11)$$

2.3 Equation of motion

Based on the Newton's second law of motion, the equations of motion for a rigid body are derived. Conventionally, the equation of motion is given as

$$\{M\}[\ddot{x}_G] + \{K\}[x_G] = [F(t)] \quad (12)$$

where

$$[M] = [M_{structure}] + [M_{added}] \quad (13)$$

$$[K] = [K_{structure}] + [K_{Mooring}] \quad (14)$$

The mass matrix, $[M]$ is expressed in Eq. (15).

$$[M] = \begin{bmatrix} m & 0 & 0 \\ 0 & m & 0 \\ 0 & 0 & I \end{bmatrix} + \left\{ \begin{bmatrix} m_{11,c} & m_{12,c} & m_{13,c} \\ m_{21,c} & m_{22,c} & m_{23,c} \\ m_{31,c} & m_{32,c} & m_{33,c} \end{bmatrix} + \begin{bmatrix} m_{11,p} & m_{12,p} & m_{13,p} \\ m_{21,p} & m_{22,p} & m_{23,p} \\ m_{31,p} & m_{32,p} & m_{33,p} \end{bmatrix} \right\} \quad (15)$$

where m = body mass and I = mass moment of inertia at y-axis.

Further in detail, the added mass was computed by integrating it from mean sea level to the keel of the structure. In this study, two components were considered for the semisubmersible platform model, such as the column and the pontoon. The added mass components for the columns and pontoons are given as in Eq. (16 ~ 27).

$$m_{11,c} = \rho \frac{\pi D,c}{4} (C_{M,c} - 1) \cos^2 \theta \partial z \quad (16)$$

$$m_{12,c} = m_{21,c} = -\rho \frac{\pi D,c}{4} (C_{M,c} - 1) \cos \theta \sin \theta \partial z \quad (17)$$

$$m_{13,c} = m_{31,c} = -\rho \frac{\pi D,c}{4} (C_{M,c} - 1) z \cos \theta \partial z \quad (18)$$

$$m_{22,c} = \rho \frac{\pi D,c}{4} (C_{M,c} - 1) \sin^2 \theta \partial z \quad (19)$$

$$m_{23,c} = m_{32,c} = \rho \frac{\pi D,c}{4} (C_{M,c} - 1) z \cos \theta \partial z \quad (20)$$

$$m_{33,c} = \rho \frac{\pi D^2,c}{4} (C_{M,c} - 1) z^2 \partial z \quad (21)$$

$$m_{11,p} = \rho A_p (C_{M,p} - 1) \cos^2 \theta \partial z \quad (22)$$

$$m_{12,p} = m_{21,p} = -\rho A_p (C_{M,p} - 1) \cos \theta \sin \theta \partial z \quad (23)$$

$$m_{13,p} = m_{31,p} = -\rho A_p (C_{M,p} - 1) z \cos \theta \partial z \quad (24)$$

$$m_{22,p} = \rho A_p (C_{M,p} - 1) \sin^2 \theta \partial z \quad (25)$$

$$m_{23,p} = m_{32,p} = \rho A_p (C_{M,p} - 1) z \cos \theta \partial z \quad (26)$$

$$m_{33,p} = \rho A_p (C_{M,p} - 1) z^2 \partial z \quad (27)$$

where $C_{M,c}$ = column added mass coefficient, $C_{M,p}$ = pontoon added mass coefficient, A_p = pontoon cross section area, θ = pitch angle response, z = inclined element distance to the centre of gravity.

Total stiffness matrix is taken as a product of hydrostatic stiffness and mooring line stiffness, whereby the hydrostatic stiffness and mooring line stiffness are given as

$$[K_{hydrostatic}] = \begin{bmatrix} 0 & 0 & 0 \\ 0 & K_{22h} & K_{23h} \\ 0 & 0 & 0 \end{bmatrix} \quad (28)$$

$$[K_{mooring}] = \begin{bmatrix} K_{11m} & 0 & K_{13m} \\ 0 & 0 & 0 \\ K_{31m} & 0 & K_{33m} \end{bmatrix} \quad (29)$$

The components for the stiffness matrices are expressed in Eq. (30~34).

$$K_{22h} = \rho g A_{wn} \quad (30)$$

$$K_{23h} = \rho g \Delta G M_p \quad (31)$$

$$K_{11m} = k_x \quad (32)$$

$$K_{13m} = K_{31m} = -k_x h \quad (33)$$

$$K_{33m} = k_x h^2 \quad (34)$$

where A_{wn} = water plane area, $G M_p$ = metacentric height for pitch, Δ = vessel displacement volume, k_x = mooring line stiffness constant, h = vertical distance of fairlead to centre of gravity.

2.4 Newmark beta method

For the analysis purpose, the equations of motions discussed were solved by the Newmark beta approach. The factor, δ was taken as 0.5 with the assumption of no artificial damping. In the iteration, the exciting forces are evaluated for every time step at the corresponding model position and up to the free surface. The displacement of the structure computed for each time step is explained in Eq. 35.

$$X_{t+\Delta} = \hat{K}^{-1} \hat{F}_{t+\Delta} \quad (35)$$

where the effective stiffness matrix, $\hat{K} = K + a_0 M$.

The acceleration $\ddot{X}_{t+\Delta t}$ and velocity $\dot{X}_{t+\Delta t}$ of the platform model are given as

$$\ddot{X}_{t+\Delta t} = a_0 (X_{t+\Delta} - X_t) - a_2 \ddot{X}_t - a_3 \dot{X}_t \quad (36)$$

$$\dot{X}_{t+\Delta t} = \dot{X}_t + a_6 \ddot{X}_t + a_7 \dot{X}_{t+\Delta t} \quad (37)$$

The effective loading matrix, $\hat{F}_{t+\Delta t}$ is elaborated as

$$\hat{F}_{t+\Delta t} = F_{t+\Delta t} + M (a_0 X_t + a_2 \ddot{X}_t + a_3 \dot{X}_t) \quad (38)$$

where the constants of the Newmark beta method are given in Eq. (39~45)

$$a_0 = 1/(\alpha \Delta t^2) \quad (39)$$

$$a_1 = \delta/(\alpha \Delta t) \quad (40)$$

$$a_2 = 1/(\alpha \Delta t) \quad (41)$$

$$a_3 = (1/2\alpha) - 1 \quad (42)$$

$$a_4 = (\delta/\alpha) - 1 \quad (43)$$

$$a_5 = (\Delta t / 2) [(\delta / \alpha) - 2] \quad (44)$$

$$a_6 = \Delta t (1 - \delta) \quad (45)$$

$$a_7 = \delta \Delta t \quad (46)$$

3 WAVE TANK MODEL STUDIES

A series of wave tank model test were conducted in the offshore laboratory of Universiti Teknologi PETRONAS to investigate the dynamic responses of the six-column semisubmersible platform model. The details of the test performed are elaborated below.

3.1 Facilities and instrumentations

The model tests were carried out in the wave tank of 22m length, 10m width and 1.5m depth as shown in Fig 1. The fore and aft of the tank are equipped with the wave generator and wave absorption beach. Wave generator is connected to a remote control unit and signal generating computer to control the 16 units of individual paddles to move forward-backward to generate the desire waves.



Figure 1 Wave tank equipped with wave generator

The other instrumentations that were adopted during the tests inclusive of inclinometer mainly for inclination test, optical tracking system to measure the motions of the target, wave probe to record the wave heights, load cells to measure the mooring system loading, and accelerometer to measure the model acceleration at the desire location.

3.2 Scale and physical law of modelling

The choice of scaling factor is important as the existing experimental facilities are limited. In this study, the Froude scaling law as listed in Table 1 was adopted.

3.3 Model description

A six-column twin-hulled semisubmersible platform model with scale of 1:100 was constructed by using steel plates. The platform model was tested for multi-directional short crested waves with \cos^2 spreading function. The setup of the model test and the model used for the test are illustrated in Fig. 2 and 3.

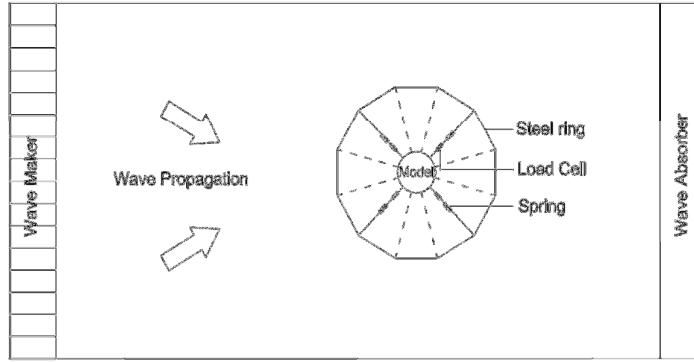


Figure 2 Experimental model setup



Figure 3 Six-column semisubmersible platform model

3.4 Wave data

In the wave generation system, multi-directional short crested wave is defined as the product of wave spectra and spreading function. Hence, in this study, spreading function \cos^2 has been taken into consideration, and the wave properties generated are tabulated in Table 2.

3.5 Post-processing of experimental measured data

Time series data were recorded by the optical tracking system during the sea-keeping test. The data were then processed by using the Discrete Fast Fourier Transformation method to obtain the responses spectra. Response spectra were obtained in terms of Response Amplitude Operator (RAO), which is given as

$$RAO = \sqrt{S_R(f)/S(f)} \quad (47)$$

where $S_R(f)$ = motion response spectrum, $S(f)$ = wave spectrum, f = wave frequency.

4 RESULTS AND DISCUSSION

The numerical estimated surge response amplitude was compared with the experimental measured record and illustrated in Fig. 4. The trend of the numerical results agreed well with the experimental results. In the figure also, it could be observed that maximum discrepancy was about 55% for surge response amplitude at 0.05Hz.

In Fig. 5, the numerical estimated heave response amplitude was compared with the experimental measured data. From the figure, the trend and magnitude of the response amplitude agreed well with maximum difference of about 34% found at the low frequency region.

The pitch response amplitude estimated numerically was compared with the experimental measured result and shown in Fig. 6. It was found that trend of the pitch response amplitude

estimated and measured was almost the same. The maximum amplitude was about 35 deg/m and 28 deg/m, for numerical estimated and experimental measured respectively. The response declined drastically at the low frequency and then gradually reduced as the wave frequency increased.

Table 1 Froude scaling law

Variable	Unit	Scale factor
Geometry		
Length	L	λ
Area	L^2	λ^2
Volume	L^3	λ^3
Angle	None	1
Radius of gyration	L	λ
Area moment of inertia	L^4	λ^4
Mass moment of inertia	ML^2	λ^5
Center of gravity	L	λ
Kinematics and dynamics		
Time	T	$\lambda^{1/2}$
Acceleration	LT^{-2}	1
Velocity	LT^{-1}	$\lambda^{1/2}$
Displacement	L	λ
Angular acceleration	T^{-2}	λ^{-1}
Angular velocity	T^{-1}	$\lambda^{1/2}$
Angular displacement	L	1
Spring constant (Linear)	MT^{-2}	λ^2
Damping coefficient	None	1
Damping factor	MT^{-1}	$\lambda^{3/2}$
Natural period	T	$\lambda^{1/2}$
Displacement	L	λ
Wave mechanics		
Wave height	L	λ
Wave period	T	$\lambda^{1/2}$
Wave length	L	λ
Celerity	LT^{-1}	$\lambda^{1/2}$
Particle velocity	LT^{-1}	$\lambda^{1/2}$
Particle acceleration	LT^{-2}	1
Water depth	L	λ
Wave pressure	$ML^{-1}T^{-2}$	λ

Table 2 Wave properties generated

Multi-directional wave		
Spreading Function	Cosine ²	
Wave Frequency, Hz	Wave Period, s	Wave Height, m
0.50	2.00	0.08
0.63	1.60	0.08
0.71	1.40	0.07
0.83	1.20	0.07
1.00	1.00	0.06
1.25	0.80	0.06

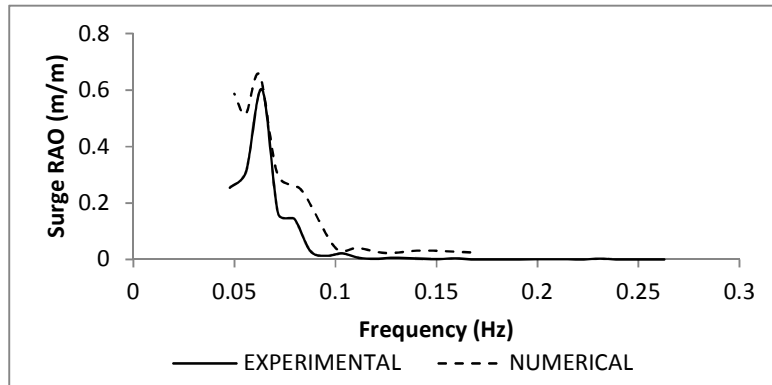


Figure 4 Surge response amplitude operator comparisons

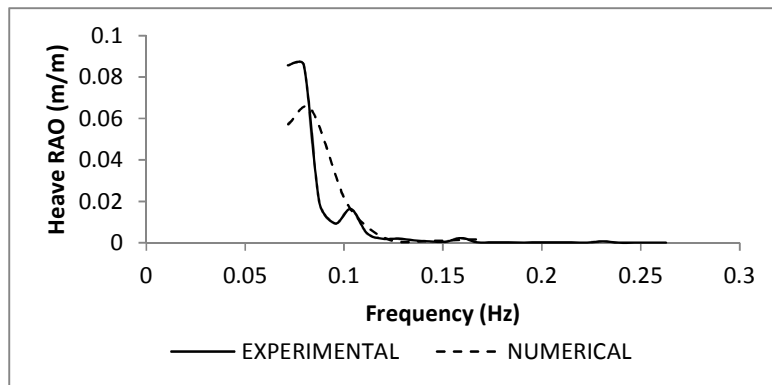


Figure 5 Heave response amplitude operator comparisons

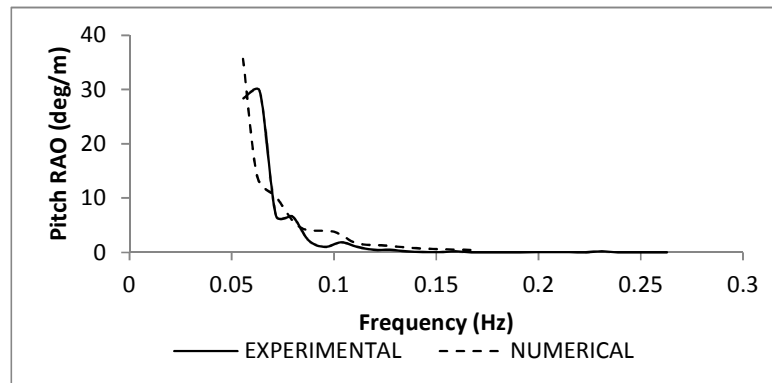


Figure 6 Pitch response amplitude operator comparisons

5 CONCLUSIONS

The response amplitudes of a six-column semisubmersible platform were estimated numerically and measured experimentally in this study. From this study, the following conclusions were drawn:

1. The numerical simulation developed was applicable to predict the responses of the six columns semisubmersible platform model fairly well. It was validated by the experimental study, where the trend and magnitude of the surge, heave and pitch responses agreed fairly well.

2. All the response amplitudes have almost similar trend of maximum response amplitude at the low frequency region. Then, it reduced gradually as the wave frequency increased.

REFERENCES

- [1] F.Z. Sun, *Analysis of motions of semi-submersible in sea waves*, OTC, 429-442, 1980
- [2] M. Soylemez, *A general method for calculating hydrodynamic forces*, Ocean Engineering, Volume 23, Issue 5, 423-445, 1996.
- [3] J.R. Paulling, Y.S. Hong, H.H. Chen and S.G. Stiansen, *Analysis of semisubmersible catamaran type platform*, Offshore Technologi Conference, Houston, Texas, May 2-5, 1977.
- [4] J. Wichers and P.V. Devlin, *Benchmark model test on the deepstar theme structures*, Offshore Technologi Conference, Houston, Texas, May 3-6, 2004.
- [5] A. Steen, M.H. Kim, M. Irani, *Prediction of spar responses: Model test vs Analysis*, Offshore Technologi Conference, Houston, Texas, May 3-6, 2004.
- [6] J. Zou, H. Ormberg, C.T. Stansberg, *Prediction of TLP responses: Model test vs Analysis*, Offshore Technologi Conference, Houston, Texas, May 3-6, 2004.
- [7] J.I. Collins and T.W. Groove, *Model test of a generic semisubmersible related to study assessing stability criteria*, Offshore Technologi Conference, Houston, Texas, May 2-5, 1988.
- [8] R. Natarajan and C.Ganapathy, *Model experiments on moored ships*, Ocean Engineering, Volume 24, Issue 7, 665 - 676, 1997
- [9] S.Zhu, *Diffraction of short-crested waves around a circular cylinder*, Ocean Engineering, Volume 20, Issue. 4, 389-407, 1993.
- [10] S.Zhu and G.Moule, *Numerical calculation of forces induced by short-crested waves on a vertical cylinder of arbitrary cross-section*, Ocean Engineering, Volume 21, Issue 7, 645-662, 1994.
- [11] S.Zhu and P.Satavaha, *Second-order wave diffraction forces on a vertical circular cylinder due to short-crested waves*, Ocean Engineering, Volume 22, Issue. 2, 135-189, 1995.
- [12] Y.Jian, J.Zhan and Q.Zhu, *Short crested wave-current forces around a large vertical circular cylinder*, European Journal of Mechanics B/Fluids 27, 346-360, 2008.
- [13] A.H.Heidari, S.M.Borghei and M.Sohrabpour, *Dynamic response of a moored semisubmersible in short-crested wave fields*, Scientia Iranica, Volume 11, No. 4, 351-360, 2004.
- [14] M.Ioualalen, M.Okamura, S.Cornier, C.Kharif and A.J.Roberts, *Computation of short-crested deepwater waves*, Journal of Waterwat, Port, Coastal, and Ocean Engineering, 2006
- [15] L.Tao, H.Song, and S.Chakrabarti, *Scaled boundary FEM model for interaction of short-crested waves with a concentric porous cylindrical structure*, Journal of Waterway Port Coast Ocean Ocean Engineering; Volume 135, Issue 5, 200-212, 2009.
- [16] J.Zhang, J.Yang, J.Wen, I.Prislin and K.Hong, *Deterministic wave model for short-crested ocean waves: Part I. Theory and numerical scheme*, Applied Ocean Research 21, 167-188, 1999.
- [17] J.Zhang, J.Yang, J.Wen, I.Prislin and K.Hong, *Deterministic wave model for short-crested ocean waves: Part II. Comparison with laboratory and field measurement*, Applied Ocean Research 21, 189-206, 1999.